Biophysical Chemistry 158 (2011) 38–45

Contents lists available at ScienceDirect

Biophysical Chemistry

journal homepage: http://www.elsevier.com/locate/biophyschem

The relationship between the structures of periphery ligands and the DNA binding mode of [Ru(II)(1,10-phenanthroline)(L_1L_2)dipyrido[3,2-*a*:2′,3′-*c*]phenazine]$^{n+}$ (L_1 = Cl or pyridine and L_2 = pyridine, n = 1,2)

Yoon Jung Jang, Ga-Young Yeo, Borami Park, Seog K. Kim *

Department of Chemistry, Yeungnam University Dae-dong, Gyeongsan City, Gyeong-buk, 712-749, Republic of Korea

ARTICLE INFO

Article history:
Received 23 February 2011
Received in revised form 22 April 2011
Accepted 22 April 2011
Available online 1 May 2011

Keywords:
Ru(II) complex
DNA
Binding mode
Light switch effect
Linear dichroism

ABSTRACT

The binding modes of the [Ru(II)(1,10-phenanthroline)(L_1L_2) dipyrido[3,2-*a*:2′,3′-*c*]phenazine]$^{2+}$ {[Ru(phen)(py) Cl dppz]$^{+}$ (L_1 = Cl, L_2 = pyridine) and ([Ru(phen)(py)$_2$dppz]$^{2+}$ (L_1 = L_2 = pyridine)} to native DNA is compared to that of the [Ru(II)(1,10-phenanthroline)$_2$dipyrido[3,2-*a*:2′,3′-*c*]phenazine]$^{2+}$ complex ([Ru(phen)$_2$dppz]$^{2+}$) by various spectroscopic and hydrodynamic methods including electric absorption, linear dichroism (LD), fluorescence spectroscopy, and viscometric titration. All measured properties, including red-shift and hypochromism in the dppz absorption band, nearly perpendicular molecular plane of the dppz ligand with respect to the local DNA helix axis, prohibition of the ethidium binding, the light switch effect and binding stoichiometry, increase in the viscosity upon binding to DNA, increase in the melting temperature are in agreement with classical intercalation of dppz ligand of the [Ru(phen)$_2$dppz]$^{2+}$ complex, in which both phenanthroline ligand anchored to the DNA phosphate groups by electrostatic interaction. [Ru(phen)(py)$_2$ dppz]$^{2+}$ and [Ru(phen)(py) Cl dppz]$^{+}$ complexes had one of the phenanthroline ligand replaced by either two pyridine ligands or one pyridine plus a chlorine ion. They exhibited similar protection from water molecules, interaction with DNA bases, and occupying site that is common with ethidium. The dppz ligand of these two Ru(II) complex were greatly tilted relative to the DNA helix axis, suggesting that the dppz ligand resides inside the DNA and is not perpendicular relative to the DNA helix axis. These observation suggest that anchoring the [Ru(phen)$_2$dppz]$^{2+}$complex by both phenanthroline is essential for the dppz ligand to be classically intercalated between DNA base-pairs.

1. Introduction

The interactions of transition metal complexes containing planar aromatic polycyclic hydrocarbon ligands with DNA have been widely studied for several decades [1]. The interactions between polypyridyl Ru(II) complexes and DNA have been of particular interest since the [Ru(1,10-phenanthroline)$_3$]$^{2+}$ that possess Δ- and Λ-enantiomers were first reported to be compatible with the helical structure of DNA [2,3]. The [Ru(1,10-phenanthroline)$_2$dipyrido[3,2-*a*:2′,3′-*c*]phenazine]$^{2+}$ complex (hereafter referred to as [Ru(phen)$_2$dppz]$^{2+}$, Fig. 1) and its derivatives, the most well-known [Ru(1,10-phenantheroline)$_3$]$^{2+}$ complex families, have also been intensively studied because of their unique photophysical properties, binding modes, and potential applications in biology [4]. One such potential application of [Ru(phen)$_2$dppz]$^{2+}$ is probing electron transfer along DNA [5–8]. More recently, [Ru(phen)$_2$dppz]$^{2+}$ has been reported to act as an acceptor in the Föster-type energy transfer reaction between 4′,6-diamidino-2-phenylindole (referred to as DAPI), a DNA minor groove binding compound, and [Ru(phen)$_2$dppz]$^{2+}$ when both were simultaneously bound to double stranded DNA [9–11]. However, it is unclear whether any electron or hole transfer accompanied this energy transfer.

Understanding the binding mode is essential for the investigation of the interactions and applications of the DNA-Ru(II)-polypyridyl complex. The binding modes of [Ru(phen)$_2$dppz]$^{2+}$ have been thoroughly studied, its expanded DPPZ ligand is known to intercalate between the DNA base-pairs [12–15], but whether the insertion is from the minor or the major groove is not yet established. In the intercalation pocket, [Ru(phen)$_2$dppz]$^{2+}$ could be stabilized by electrostatic and hydrophobic interactions or by π–π interactions between its DPPZ ligand and the DNA base-pairs. The electrostatic attraction between the two positively charged phenanthroline ligands and the negatively charged DNA phosphate groups could provide additional stabilization and form anchors for the complex. However, the exact role of the two phenanthroline ligands in the binding has not been fully elucidated. Therefore this work investigates the DNA binding modes of two Ru(II) complex derivatives, [Ru(II)(1,10-phenanthroline)(L_1L_2)dipyrido[3,2-*a*:2′,3′-*c*]phenazine]$^{n+}$ (L_1 = Cl or pyridine and L_2 = pyridine, abbreviated hereafter by [Ru(phen)(py)$_2$dppz]$^{2+}$ and [Ru(phen)(py)

* Corresponding author. Tel.: +82 53 810 2362; fax: +82 53 815 5412.
E-mail address: seogkim@yu.ac.kr (S.K. Kim).

0301-4622/$ – see front matter © 2011 Elsevier B.V. All rights reserved.
doi:10.1016/j.bpc.2011.04.014

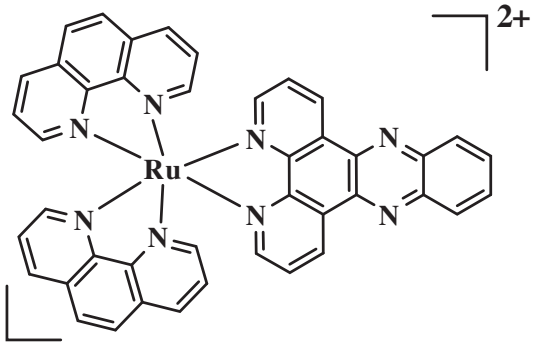

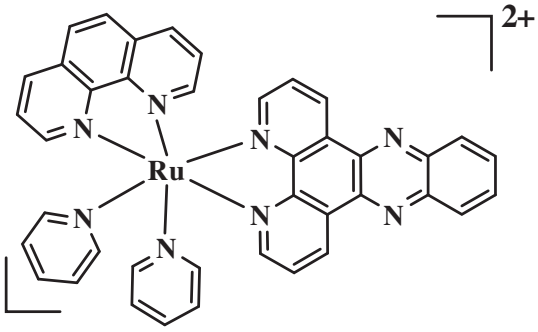

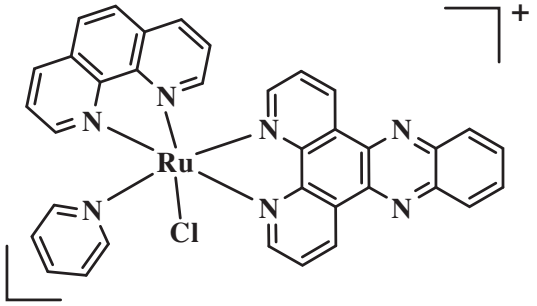

Fig. 1. Chemical structures of the Ru(II)-polypyridyl complexes.

Cl dppz]$^+$, respectively, Fig. 1). These derivatives of [Ru(phen)$_2$dppz]$^{2+}$ have one of the phenanthroline ligands replaced by either one pyridine molecule and one chloride ion or two pyridine molecules, providing flexibility for the remaining phenanthroline ligand. The effects of the flexibility and rotational ability allowed by the chloride and pyridine could provide some insight into the role of phenanthroline in anchoring.

2. Materials and methods

2.1. Syntheses of the Ru complexes

Ru(phen)$_2$Cl$_2$ and [Ru(phen)$_2$dppz]$^{2+}$ were synthesized by elsewhere reported methods [13,16]. [Ru(phen)(py)$_2$dppz]$^{2+}$ and [Ru(phen)(py)Cl dppz]$^+$ were synthesized in a similar way to Ru(phen)$_2$Cl$_2$. First, RuCl$_3$·H$_2$O (1 mmol, 0.2254 g) was dissolved in 10 mL DMF and solutions of DMF containing pyridine (2 mmol, for [Ru(phen)(py)$_2$dppz]$^{2+}$ or 1 mmol, for [Ru(phen)(py) Cl dppz]$^+$) in the presence of 1 mmol phenanthroline and excess LiCl were added. The solutions were heated under reflux for 24 h and 12 h, respectively. The reaction mixtures were then cooled to room temperature, 70 ml reagent grade acetone was added to each, and the resulting solutions were cooled at −20 °C overnight. A red-to-violet colored solution and a dark red product were obtained after filtration. The solid was washed several times with cold acetone and water. The crude product was suspended in 50 ml hot ethanol, and 50 ml water was added. The solution was boiled until it was completely dissolved. (The solution was filtered hot and 12 g LiCl was added carefully with stirring only for ru–py). The ethanol was removed through evaporation during recrystallization. The reddish products were removed by filtration and washed first with cold water and then several times with diethyl ether. The reddish-orange solid was dissolved in water, to which an aqueous ammonium hexafluorophosphate solution was added to produce another reddish-orange solid, which was filtered, washed with diethylether and dried in a dry oven at 50 °C. The orange solid was dissolved in acetonitrile and chromatographed on alumina (20×1 cm) with acetonitrile eluent. The orange band was collected, and column separation was repeated for higher purity. The orange solution was concentrated by evaporation and then solidified with diethylether. The light reddish-orange solid was collected by filtration, washed with diethylether, and dried in a dry oven at 50 °C. The solid was then dissolved in acetone, and tetrabutylammonium chloride in acetone was added to obtain a water-soluble compound. The light reddish-orange solid was filtered, washed with diethylether and dried in a dry oven at 50 °C. All solvents were dried by standard procedures prior to use. All reactions were carried out under an inert atmosphere.

[Ru(phen)$_2$dppz]$^{2+}$

[Ru(phen)$_2$dppz](PF$_6$)$_2$yield 100mg

Elemental analysis calcd(%) for C$_{42}$H$_{26}$N$_8$P$_2$F$_{12}$Ru (1033.713): C 48.80, H 2.54, N 10.84; found: C 48.00, H 2.43, N 11.03.

^{1}H NMR ([Ru(phen)$_2$dppz]Cl$_2$, 600 MHz, DMSO-*d*6, 25 °C): δ = 9.64 (dd, 4H), 8.80 (m, 2H), 8.53 (d, 2H), 8.40 (dd, 2H), 8.25 (m, 6H), 8.20 (m, 2H), 8.07 (d, 2H), 7.91 (dd, 2H), 7.81 (dd, 2H), 7.78 (dd, 2H).

[Ru(phen)(py)$_2$dppz]$^{2+}$: yield 90mg

[Ru(phen)(py)$_2$dppz](PF$_6$)$_2$

Elemental analysis calcd(%) for C$_{40}$H$_{28}$N$_8$P$_2$F$_{12}$Ru (1011.7068): C 47.49, H 2.79, N 11.08; found: C 47.59, H 3.00, N 10.99.

^{1}H NMR ([Ru(phen)$_2$(py)$_2$dppz]Cl$_2$, 600 MHz, DMSO-*d*6, 25 °C): δ = 9.75 (d, 2H), 9.68 (dd, 4H), 8.84 (m, 2H), 8.58 (d, 2H), 8.43 (m, pyH), 8.39 (dd, 2H), 8.28 (m, 3H), 8.23 (m, 2H), 8.15 (d, 1H), 7.82 (dd, 2H), 7.65 (m, pyH), 7.64 (dd, 1H), 7.33 (dd, 1H).

[Ru(phen)(py)Cldppz]$^+$: yield 105mg

[Ru(phen)(py)dppzCl]PF$_6$·2H$_2$O

Elemental analysis calcd(%) for C$_{35}$H$_{27}$N$_7$O$_2$ClPF$_6$Ru (859.1272): C 48.93, H 3.17, N 11.41; found: C 48.59, H 2.61, N 11.29.

^{1}H NMR ([Ru(phen)(py)dppzCl]Cl, 600 MHz, DMSO-*d*6, 25 °C): δ = 9.64 (dd, 4H), 8.78 (m, 2H), 8.52 (d, 2H), 8.41 (m, pyH), 8.38 (dd, 2H), 8.26 (m, 3H), 8.20 (m, 2H), 8.04(d, 1H), 7.93 (dd, 2H), 7.89(m, pyH), 7.79(dd, 1H), 7.76(dd, 1H).

2.2. Other materials

All chemicals, including calf thymus DNA, were purchased from Sigma-Aldrich and used without further purification except for the DNA, which was further purified by an elsewhere reported method [17].

5 mM cacodylate buffer of pH 7.0 was used throughout. Concentrations were spectrophotometrically determined using extinction coefficients of $\varepsilon_{260\ nm} = 6700\ M^{-1}cm^{-1}$, $\varepsilon_{440\ nm} = 20{,}000\ M^{-1}cm^{-1}$, $9560\ M^{-1}cm^{-1}$, $16{,}950\ M^{-1}cm^{-1}$ for DNA, $[Ru(phen)_2dppz]^{2+}$, $[Ru(phen)(py)_2dppz]^{2+}$, and $[Ru(phen)(py)\ Cl\ dppz]^{+}$, respectively. The extinction coefficients of aqueous ethidium bromide and DAPI were $5800\ M^{-1}cm^{-1}$ at 480 nm and $27{,}000\ M^{-1}cm^{-1}$ at 342 nm, respectively.

2.3. Spectroscopic measurements

Absorption spectra were recorded on a Cary 100 spectrophotometer (Varian, Australia) and all luminescence measurements were performed on a Jasco FP-777 fluorimeter (Jasco, Japan). Linear dichroism (LD) was carried out using a Jasco J715 spectropolarimeter equipped with a Wada type inner-rotating flow cell to align the DNA samples [18]. The general principles, technique, and application of LD for nucleic acid were as described by Nordén et al. [19–21]. The application of LD to DNA-Ru(II)-polypyridyl complexes, especially $[Ru(phen)_2dppz]^{2+}$ and its derivatives, is also well established [13,22–24]. In short, the measured LD is divided by the isotropic absorption spectrum to determine the wavelength-dependent dimensionless quantity of reduced linear dichroism, LD^r, which is related to the angle, α, of the electric transition moment of any DNA-bound drug with respect to the local DNA helix axis (flow direction in the flow orientation system) by:

$$LD^r = 1.5S\left(<3\ cos^2\alpha > -1\right)$$

In this equation, the orientation factor, S, can be determined from the LD^r at 260 nm, assuming the average angle of 86° between the DNA base and the DNA helix when the contribution of the DNA-bound drug was negligible.

2.4. Viscosity measurement

The cubic ratio of the viscosity in the presence of the drug, η, to the viscosity in the absence of drug, η^0, is related to the length of the DNA in the absence (L_0) and presence (L) of drug by [14,25,26]:

$$\frac{L}{L_0} = \left(\frac{\eta}{\eta^0}\right)^{1/3}$$

Relative viscosities were obtained by observing flow times of the DNA-containing solutions (t) that were corrected for the flow time of buffer (t_0) using conventional Ubbelohde-type viscometry at 25 °C, as reported for $[Ru(phen)_2L]^{2+}$ complexes [14]. The reported values are averages of nine measurements. The DNA used in the viscosity measurements was sonicated.

2.5. Melting profiles

The dissociation of DNA from its double strand produced hyperchromism in the 260 nm wavelength region. The melting profiles were measured using a Cary 100 spectrophotometer. The temperature was increased at 0.5 °C/min, and readings were taken 3 min after each temperature increase. The results are displayed as increases in absorbance per temperature change, i.e., dA/dT with respect to temperature.

3. Results

3.1. Absorption spectrum

The absorption spectra of the aqueous Ru(II) complexes showed large $\pi \rightarrow \pi^*$ intra-ligand transition bands at wavelengths of 200–300 nm and several $d \rightarrow \pi^*$ metal to ligand charge transfer (referred to as MLCT) transitions above 400 nm. Absorption at 300–400 nm was assigned to the $\pi \rightarrow \pi^*$ intra-ligand electric transitions polarized along the long and short symmetry axes of the dppz ligand [13,23,24]. In the absence of DNA, the absorbance ratio at the maximum of the MLCT band to the dppz absorption band was 0.91 for the $[Ru(phen)_2dppz]^{2+}$ complex, whereas this ratio became 0.60 and 0.71 for $[Ru(phen)(py)_2dppz]^{2+}$ and $[Ru(phen)(py)\ Cl\ dppz]^{+}$, respectively (Fig. 2), reflecting the effect on relative charge transfer of replacing one of the phenanthroline ligands with pyridine or chlorine. Hypochromism and red-shift were apparent in all the absorption bands after binding with DNA. They were particularly pronounced in the dppz absorption region. The red-shifts of the absorption maximum at 372 nm were 7 nm, 7 nm, and 4 nm and the hypochromisms were 18.9%, 36.2% and 28.5% for $[Ru(phen)_2dppz]^{2+}$ (Fig. 2a), $[Ru(phen)(py)_2dppz]^{2+}$ (Fig. 2b), and $[Ru(phen)(py)\ Cl\ dppz]^{+}$ (Fig. 2c), respectively. These observations were typical for intercalating drugs and suggested strong interactions between the dppz ligands and the DNA bases. The change in the MLCT band for the $[Ru(phen)_2dppz]^{2+}$ complex was relatively small, however significant hypochromism was observed in $[Ru(phen)(py)_2dppz]^{2+}$ and $[Ru(phen)(py)\ Cl\ dppz]^{+}$. Finally, absorption spectra of the DNA-Ru(II) complex adducts for [Ru(II) complex]/[DNA base] ratios below 0.1 were identical across the entire absorption wavelength when the absorption spectrum of free DNA was subtracted from that of the Ru(II) complex-DNA adduct, and normalized to the highest mixing ratio. This observation indicated that the binding mode was independent of mixing ratio, and the amount of unbound Ru(II) complex was negligible under the conditions used in this study.

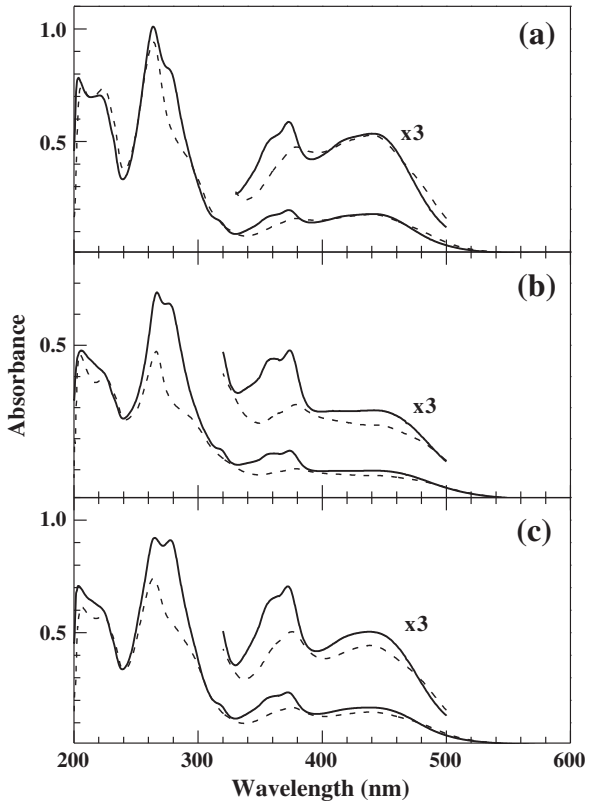

Fig. 2. Absorption spectrum of (a) $[Ru(phen)_2dppz]^{2+}$, (b) $[Ru(phen)(py)_2dppz]^{2+}$, and (c) $[Ru(phen)(py)\ Cl\ dppz]^{2+}$ in the presence (dashed curve) and absence (solid curve) of DNA. [DNA] = 100 μM, [Ru(II) complexes] = 10 μM. The shapes of absorption spectra at low [Ru(II) complex]/[DNA] concentrations (2, 4, 6, 8 μM Ru(II) complex) were identical when they were normalized to the highest concentration (10 μM), and hence they are not shown. The absorption spectrum of DNA was subtracted from the DNA-Ru(II)-pyridyl complex adduct for ease of comparison.

3.2. Reduced linear dichroism

Drugs that bind at the minor groove of DNA produce positive LD^r signals at the wavelength range corresponding to the absorption of the in-plane electric transition moment. The magnitude of LD^r is expected to match the angle of $\alpha = 45°$, which is the angle of the minor groove with respect to the DNA helix axis, if the absorption envelope represents one electric transition moment polarized along the groove [27–29]. On the other hand, the electric transition moments of an intercalated drug usually appear to be negative, and the magnitude of LD^r is either comparable to or larger than the DNA absorption region [27,30]. The LD^r spectra of the DNA-bound Ru(II) complexes (Fig. 3) show that each LD^r signal in the DNA absorption region (240–300 nm) was negative, as expected from the set-up adopted in this study [17–21]. All the complexes showed decreasing LD^r magnitudes in the DNA absorption region as the concentration of the Ru(II) complex increased, suggesting either decreased orientation ability of the DNA stem or significant positive contribution from the Ru(II) complex. The second explanation was considered more conceivable because viscosity increased as the [Ru(II) complex]/[DNA base] ratio increased in all cases, implying increased DNA contour length (see below). The positive contribution to the LD^r magnitude was significant in the ~260 nm region. Therefore, LD^r intensity at 240 nm was used to calculate *S* values because positive contributions from the ligands were less significant than at 260 nm. Changing the wavelength from which *S* values were calculated did not affect the resulting α angles or the qualitative discussion below. The angles were 72°–77° at 310 nm, 79°–86° at 330 nm, and 60°–62° at 370 nm for $[Ru(phen)_2dppz]^{2+}$. In the lamellar liquid crystal, the absorption at 318 nm corresponded to the B(sh) polarized transition (in-plane, along the short symmetric axis of dppz); absorption at 301–306 nm represented the A polarized transition (in-plane, along the long symmetric axis of dppz) [24]. The first two absorption bands at 310 nm and 330 nm for DNA-bound $[Ru(phen)_2dppz]^{2+}$ represented the B(sh) and A polarized transitions, respectively. These bands were red-shifted likely due to differences in the nature of the medium. Therefore, the molecular plane of the dppz ligand was near parallel (perpendicular to the local DNA helix axis), confirming the intercalation of the dppz ligand of $[Ru(phen)_2dppz]^{2+}$ upon binding to DNA. The absorption band near 370 nm overlapped with the positive MLCT band [22], and could therefore not give any definite information about the binding geometry of $[Ru(phen)_2dppz]^{2+}$. A shoulder and small band appeared at 310 and 333 nm, respectively, for $[Ru(phen)(py)_2dppz]^{2+}$. The angles were 63°–64° and 53°–54° for the in-plane $\pi \rightarrow \pi^*$ transition moments that were respectively perpendicular and parallel to the molecular long symmetric axis of the dppz ligand, with respect to the local DNA helix axis. A very strong tilt in the transition moments of $[Ru(phen)(py)\ Cl\ dppz]^{+}$ was observed. The angles for the B(sh) and A polarized transitions of the complex were 60°–66° and 55°–62°, respectively, indicating that the molecular plane strongly tilted relative to the local DNA helix axis.

When ethidium, a typical intercalator, bound to DNA, the LD signal in the ethidium absorbing region was expected to be negative and proportional to the concentration of DNA-bound ethidium. In Fig. 4, the LD magnitude of the ethidium–DNA adduct at 520 nm proportionally increased until the [ethidium]/[DNA base] ratio reached *ca.* 0.2. At higher ethidium concentrations, the rate of increase was lower – in accordance with the neighboring site exclusion model of intercalation. When the same titration was performed with DNA already bound with the Ru(II) complexes at [Ru(II) complex]/[DNA base] ratios of 0.25, the increase in the LD magnitude of ethidium was significantly less pronounced, suggesting that the intercalation site for ethidium was already occupied or distorted by the Ru(II) complexes. When the minor groove of DNA was blocked by DAPI [31], there was a moderate increase in LD magnitude, suggesting that blocking the minor groove did not completely prevent the ethidium intercalation.

3.3. Luminescence measurement – light switch effect and Job plots

The fluorescence intensity of ethidium increases upon its binding to DNA, a good diagnostic of its intercalation between DNA base pairs. Fig. 5 shows fluorescence intensity in the presence and absence of

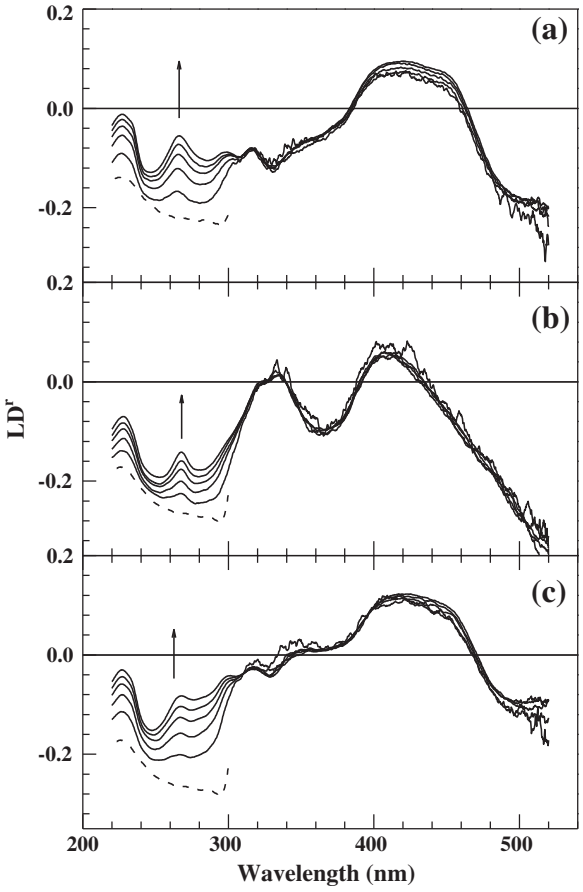

Fig. 3. LD^r spectra of (a)$[Ru(phen)_2dppz]^{2+}$, (b) $[Ru(phen)(py)_2dppz]^{2+}$, and (c) $[Ru(phen)(py)\ Cl\ dppz]^{2+}$ associated with DNA. The spectrum of Ru(II) complex-free DNA is shown by the dashed curve. [DNA] = 100 μM. The concentrations of the Ru(II) complexes (2, 4, 6, 8, and 10 μM) increased in the direction of the arrow.

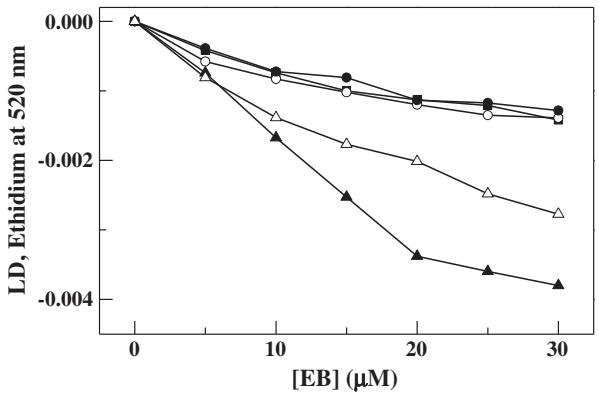

Fig. 4. Increase in LD intensity at 520 nm with respect to concentration upon association of ethidium with DNA (closed triangles), and that in the presence of DAPI (open triangles) and the DNA-Ru(II) complexes. The closed and open circles denote the DNA-$[Ru(phen)(py)\ Cl\ dppz]^{+}$ and DNA-$[Ru(phen)(py)_2dppz]^{2+}$ complexes, respectively. The closed squares represent DNA-$[Ru(phen)_2dppz]^{2+}$. [DNA] = 100 μM, [DAPI] = [Ru(II) complexes] = 25 μM.

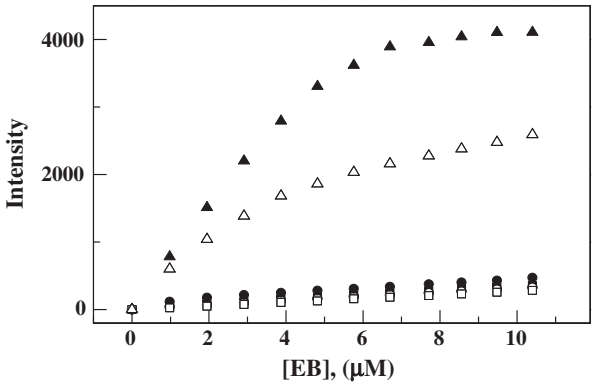

Fig. 5. Increase in luminescence intensity of ethidium upon association with DNA, and DNA adducts with DAPI, [Ru(phen)(py) Cl dppz]$^{2+}$, [Ru(phen)(py)$_2$dppz]$^{2+}$, and [Ru(phen)$_2$dppz]$^{2+}$. [DNA] = 30 μM. [DAPI] = [Ru(II) complexes] = 7.5 μM. Excitation wavelength, 530 nm; emission wavelength, 600 nm. Slit widths were 10 nm for both excitation and emission. The symbols assigned as per Fig. 4. DNA-free ethidium is denoted by open squares.

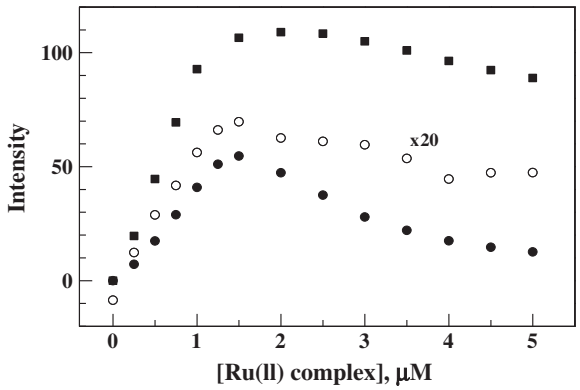

Fig. 6. Increase in the luminescence intensity of the Ru(II) complexes with respect to concentration in the presence of DNA. Excitation wavelength, 440 nm; emission wavelength, 606 nm. Slit widths were 10 nm for both excitation and emission. The closed and open circles denote DNA-[Ru(phen)(py) Cl dppz]$^{2+}$ and DNA-[Ru(phen)(py)$_2$dppz]$^{2+}$, respectively. The closed squares represent the DNA-[Ru(phen)$_2$dppz]$^{2+}$ complex. [DNA] = 5 μM. The intensities of the [Ru(phen)(py)$_2$dppz]$^{2+}$ complex were amplified 20× times for comparison.

DNA as well as in the presence of DNA-[Ru(phen)$_2$dppz]$^{2+}$, DNA-[Ru(phen)(py)$_2$dppz]$^{2+}$, DNA-[Ru(phen)(py) Cl dppz]$^{+}$, and DNA-DAPI adducts at [Ru(II) complex]/[DNA base] or [DAPI]/[DNA base] ratios of 0.25. In the presence of DNA without any drug, the fluorescence intensity of ethidium almost proportionally increased up to a concentration of 6 μM, corresponding to an [ethidium]/[DNA base] ratio of 0.2. However, the concentration dependence of fluorescence intensity was almost negligible in the absence of DNA on a similar scale. A similar fluorescence intensity trend was observed when the DNA was already saturated with the Ru(II) complexes. When DAPI occupied the minor groove of the DNA, the increase in the fluorescence intensity of ethidium was far more pronounced than when DNA was bound with the Ru(II) complexes, but less pronounced than when the DNA was drug-free. This observation is in agreement with the results from LD measurement (Fig. 4).

Although the quantum yield of aqueous [Ru(phen)$_2$dppz]$^{2+}$ was negligibly small, the luminescence intensity increased greatly upon binding to DNA [5–8]. This phenomenon is known as the "light switch effect". This effect was used as an indication of dppz intercalation because it is caused by the removal of the water molecules surrounding the [Ru(phen)$_2$dppz]$^{2+}$ complex. The luminescence intensity of the complex gradually increased as it bound to the DNA (Fig. 6). The maximum intensity was reached at a mixing ratio of 0.25–0.3. Any further increase in the mixing ratio slightly decreased luminescence intensity through self-quenching. [Ru(phen)(py) Cl dppz]$^{+}$ exhibited a similar behavior although the maximum intensity was half that of when [Ru(phen)$_2$dppz]$^{2+}$ was used and the decrease of luminescence intensity was more pronounced at high concentrations. The luminescence intensity of [Ru(phen)(py)$_2$dppz]$^{2+}$ changed very little upon binding to DNA. However, magnifying intensity 20× allowed a similar pattern to be observed, where the luminescence intensity gradually increased up to a mixing ratio of 0.25–0.30, before slightly decreasing at higher concentrations. The maximum luminescence intensity of [Ru(phen)(py)$_2$dppz]$^{2+}$ was almost one-twentieth that of [Ru(phen)(py) Cl dppz]$^{+}$. Differences in light switching – or the extent of the complexes' water-exposure – were not the only reasons for the different maximum intensities. Rather, the differences in the intensities could be attributable to differences in the natures of the three complexes. In EtOH, the luminescence intensity of [Ru(phen)$_2$dppz]$^{2+}$ was the highest, with [Ru(phen)(py) Cl dppz]$^{+}$ and [Ru(phen)(py)$_2$dppz]$^{2+}$ showing 0.9 and 0.03 of its value, respectively (data not shown).

The binding stoichiometry of the Ru(II) complexes was determined from Job plots. The complexes' absorption spectra and luminescence properties suggest that their binding modes were homogeneous, thus the changes of luminescence intensity were used to determine the binding stoichiometry. Clear luminescence maxima were observed at 0.25 mol fractions of each Ru(II) complex (Fig. 7). When the dppz ligand of [Ru(phen)$_2$dppz]$^{2+}$, similarly with ethidium, intercalated between the DNA base-pairs, a binding stoichiometry of one dppz ligand per four DNA bases or two base-pairs was expected from the "nearest neighboring site exclusion model". Similar binding stoichiometry was observed for [Ru(phen)(py) Cl dppz]$^{+}$ and [Ru(phen)(py)$_2$dppz]$^{2+}$, although the maximum for the latter complex was less clear.

3.4. Thermal melting profile and viscosity measurements

Dissociation of double-stranded DNA into two single strands results in significant hyperchromism at *ca.* 260 nm. In this study, DNA exhibited a melting temperature, T_m, of 60.7 °C at the current ionic strength (Fig. 8). The addition of [Ru(phen)$_2$dppz]$^{2+}$, [Ru(phen)(py)$_2$dppz]$^{2+}$, and [Ru(phen)(py) Cl dppz]$^{+}$ at [Ru(II) complex]/[DNA base] ratios of 0.05 increased T_m to 65.0 °C, 63.6 °C and 64.0 °C, respectively. This increase was slightly larger than the increase observed with minor groove drug binding and was similar to that observed for ethidium.

The intercalation of any drug between the base-pairs of DNA can unwind its helical structure, stiffening and increasing its contour length and as a result, increase its viscosity. Therefore, increases of viscosity are generally indicative of drug intercalation between DNA

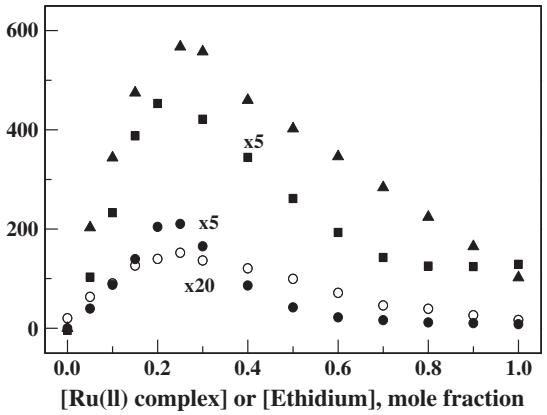

Fig. 7. Job plots for the association of the Ru(II) complexes with DNA. The highest concentration of DNA was 5 μM. The conditions for luminescence intensity detection and the curves' symbols are as per Fig. 7.

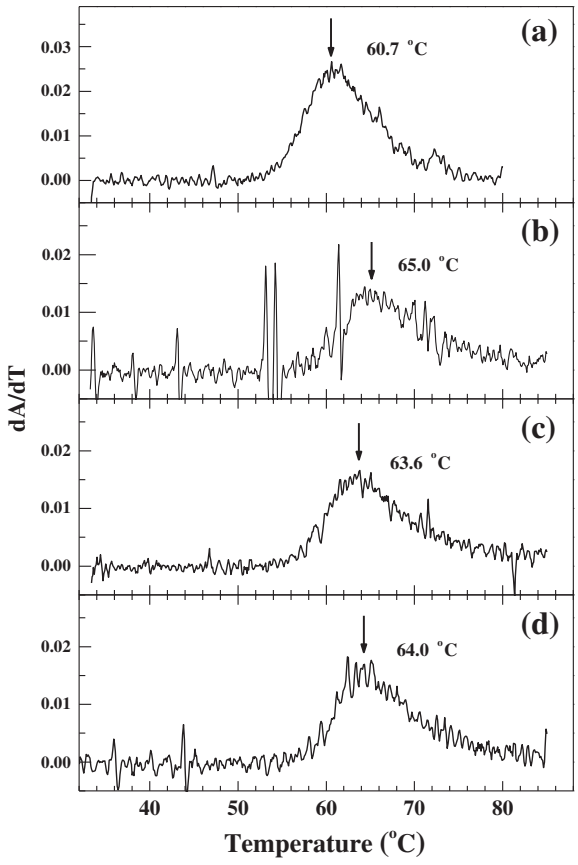

Fig. 8. Thermal melting profiles of (a) the DNA and (b) DNA-$[Ru(phen)_2dppz]^{2+}$, (c) DNA-$[Ru(phen)(py)_2dppz]^{2+}$, and (d) DNA-$[Ru(phen)(py)\ Cl\ dppz]^{2+}$. [DNA] = 100 μM and [Ru(II) complex] = 5 μM.

base-pairs. Relative viscosity increased with increased loadings of the Ru(II) complexes (Fig. 9), indicative of increased DNA contour length. This effect was most pronounced with $[Ru(phen)_2dppz]^{2+}$. The maximum viscosity reached was 1.4× that of the original DNA. The $[Ru(phen)(py)_2dppz]^{2+}$ complex exhibited the lowest relative viscosity, with a maximum value of 1.1. Maximum viscosities were observed at [Ru(II) complex]/[DNA] ratios of 0.15–0.2.

4. Discussion

4.1. Binding stoichiometry and the light switch effect

The light switch effect is considered an indication of dppz intercalation because it arises from the removal of water molecules surrounding the $[Ru(phen)_2dppz]^{2+}$ complex. It was observed in the $[Ru(phen)(py)_2dppz]^{2+}$ and $[Ru(phen)(py)\ Cl\ dppz]^{+}$ complexes, at a mixing ratio of ~0.3 giving maximum luminescence intensity in both cases. This was similar to $[Ru(phen)_2dppz]^{2+}$, suggesting that both of the former complexes saturated the DNA at similar binding ratios. However, the maximum luminescence intensities were distinctly different. The luminescence intensity of $[Ru(phen)_2dppz]^{2+}$ when bound to DNA was approximately twice that observed with $[Ru(phen)(py)\ Cl\ dppz]^{+}$ and *ca.* 30× that shown by $[Ru(phen)(py)_2dppz]^{2+}$. These differences were attributable at least in part to differences in their quantum yields when in a non-polar environment. In EtOH, the luminescence intensities of $[Ru(phen)(py)\ Cl\ dppz]^{2+}$ and $[Ru(phen)(py)_2dppz]^{2+}$ were respectively 0.9 and 0.03 of that shown by $[Ru(phen)_2dppz]^{2+}$. Therefore, differences in the complexes' natures were behind the differences in intensity maxima, rather than differing extents of exposure to polar water molecules.

Ethidium is a well known intercalator. The Job plots showed that the binding stoichiometry was one ethidium per four DNA bases or two base-pairs, in agreement with the "nearest neighboring group exclusion model" of drug intercalation. Similar binding stoichiometries were observed for all three Ru(II) complexes, indicating that their binding stoichiometries were identical to ethidium. A second complex formation was observed for all the Ru(II) complexes at a 1–2:1 ligand-to-DNA base concentration ratio, consistent with results reported by Haq et al. [14] for the Δ- and Λ-enantiomers of $[Ru(phen)_2dppz]^{2+}$. These results may have corresponded to a second, low affinity, binding mode based on the luminescence titration experiments by Hirot et al. [13].

4.2. Extrusion of intercalator

The equilibrium constant for $[Ru(phen)_2dppz]^{2+}$ with DNA in a comparable ionic strength (10 mM NaCl and 1 mM sodium cacodylate buffer) was reported to be in the range of $10^7\ M^{-1}$ [13]. The shape of the absorption spectrum did not vary with mixing ratio for all the Ru(II) complexes, indicative of equally high equilibrium constants for $[Ru(phen)(py)\ Cl\ dppz]^{+}$ and $[Ru(phen)(py)_2dppz]^{2+}$. The LD and fluorescence measurements confirmed that the intercalation of ethidium was prohibited because the intercalation pockets were already occupied or distorted by the strongly bound dppz ligands of the Ru(II) complexes. The magnitude of the negative LD signal and the fluorescence intensity of ethidium were expected to increase upon binding to the DNA. However, the increases of both signals were significantly less pronounced when the DNA was associated with the Ru(II) complexes, suggesting that the presence of the dppz ligand inhibited the binding of ethidium. On the other hand, pronounced increases of the LD magnitude and the fluorescence intensity of ethidium upon binding to DNA in the presence of DAPI suggested that minor groove binding drug molecules did not completely suppress the intercalation of ethidium. Ethidium intercalation was inhibited by the Ru(II) complexes because either the intercalation pockets of the DNA were occupied by dppz ligands of the Ru(II) complexes or their conformations were altered as a result of the Ru(II) complexes binding to the DNA, which indirectly prohibited ethidium binding. For $[Ru(phen)_2dppz]^{2+}$, the binding geometry and viscosity measurements showed that ethidium binding was inhibited because the intercalation sites were occupied by the extended dppz ligand (see below). However, the reason for inhibition by $[Ru(phen)(py)\ Cl\ dppz]^{+}$ and $[Ru(phen)(py)_2dppz]^{2+}$ was unclear because not all the binding geometry and viscosity measurements supported the classical intercalation of the dppz ligand.

4.3. Interaction with DNA bases and elongation

The large red-shifts and hypochromism observed in the absorption bands of the drugs upon intercalation of the at least partially-fused, aromatic compounds to DNA were attributed to π–π interactions between the planar intercalators and the DNA bases. For the minor groove binding drug, the red-shift resulted from conformational changes in the drug. For $[Ru(phen)_2dppz]^{2+}$, the large red-shift and hypochromism, particularly in the dppz absorption region, were attributed to π–π interactions between the DNA bases and the intercalated dppz ligands. Similar red-shift and hypochromism were observed for $[Ru(phen)(py)\ Cl\ dppz]^{+}$ and $[Ru(phen)(py)_2dppz]^{2+}$, suggestive of similar π–π interactions. In the MLCT absorption region, the decrease of absorption upon binding to DNA was more pronounced for $[Ru(phen)(py)\ Cl\ dppz]^{+}$ and $[Ru(phen)(py)_2dppz]^{2+}$ than for $[Ru(phen)_2dppz]^{2+}$, suggesting that the interactions of the ligands with the DNA were different, as expected from the ligands' structures. The 3°–5° increase in T_m also confirmed the strong interactions between the dppz ligands and the DNA bases. An increase in relative viscosity is generally accepted as indicative of classical intercalation [25,26]. The relative viscosity of the DNA increased as the concentration of [Ru

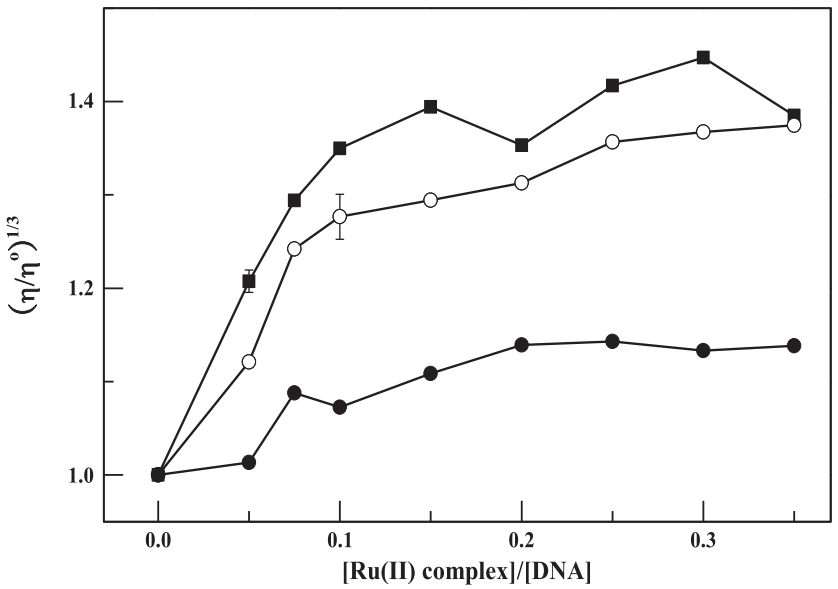

Fig. 9. The relative viscosity with respect to the mixing ratio for DNA-$[Ru(phen)_2dppz]^{2+}$ (closed squares), DNA-$[Ru(phen)(py)_2dppz]^{2+}$ (open circles), and DNA-$[Ru(phen)(py)\ Cl\ dppz]^{2+}$ (closed circles). Data were the averages of 9 measurements. The representative standard deviations from the 9 measurements are shown. Sonicated DNA was used for these measurements.

$(phen)_2dppz]^{2+}$ increased, as already reported for the Δ- and Λ-enantiomers of the complex [14]. The gradual increase in viscosity neared a maximum at a [Ru(II) complex]/[DNA base] ratio of 0.15. At higher concentrations of the complex, the extent of the increase was less. The maximum relative viscosity ratio was 1.4, in agreement with the value reported by Haq et al. [14]. Therefore, the dppz ligand of $[Ru(phen)_2dppz]^{2+}$ intercalated between the DNA bases. A similar increase was observed for $[Ru(phen)(py)\ Cl\ dppz]^{+}$, indicating that elongation with this complex was as effective as with $[Ru(phen)_2dppz]^{2+}$. However, elongation by $[Ru(phen)(py)_2dppz]^{2+}$ was significantly less, with the maximum value slightly higher than 1.1, obviously deviating from classical intercalation.

4.4. Tilt angle of dppz ligand and binding mode

If the dppz ligand intercalates between DNA base-pairs, its molecular plane is expected to be nearly perpendicular to the local DNA helix axis and parallel to the DNA base planes. The corresponding angle of both the long and short axis transition moments is *ca.* 86° with respect to the local DNA helix axis. The calculated angles were 72°–77° for the in-plane transition along the long symmetric axis of the dppz ligand and 79°–86° along the short axis for $[Ru(phen)_2dppz]^{2+}$, in accordance with classical intercalation of the dppz ligand. However, the respective tilt angles of 55°–62° and 53°–54° between the long axis of the dppz ligand and the DNA helix axis for $[Ru(phen)(py)\ Cl\ dppz]^{+}$ and $[Ru(phen)_2dppz]^{2+}$ certainly deviated from the classical intercalation binding mode. The LD^r spectrum of $[Ru(phen)_2dppz]^{2+}$ resembled that of $[Ru(phen)(py)\ Cl\ dppz]^{+}$ and was significantly different from that of $[Ru(phen)(py)_2dppz]^{2+}$ above 400 nm, which corresponded to MLCT transitions with complicated directions.

Many results confirmed that the dppz ligands of $[Ru(phen)_2dppz]^{2+}$ intercalated between the DNA base-pairs, including the red-shift and hypochromism in the dppz absorption band, the nearly perpendicular molecular plane of the dppz ligand with respect to the local DNA helix axis, the prohibition of ethidium binding, the light switch effect, the binding stoichiometry, and increases of viscosity and melting temperature upon binding to the DNA. Similar results were observed for both $[Ru(phen)(py)\ Cl\ dppz]^{+}$ and $[Ru(phen)(py)_2dppz]^{2+}$, including similar extents of the protection from water molecules (light switch effects), similar interactions with DNA bases, and the common occupying site with ethidium. However, important differences were also observed. The tilt angle of the dppz ligand of $[Ru(phen)(py)\ Cl\ dppz]^{+}$ and $[Ru(phen)(py)_2dppz]^{2+}$ did not support the intercalative binding of these complexes. Additionally, when $[Ru(phen)(py)\ Cl\ dppz]^{+}$ bound to the DNA, the elongation of the DNA was significantly lower than when the other two complexes were bound, which also did not correspond to intercalative binding. These observations suggest that the binding mode of these two complexes greatly deviated from the classical intercalation of dppz that was observed for $[Ru(phen)_2dppz]^{2+}$. The increase in luminescence intensity and the large tilt of the dppz ligand were understandable if the $Ru(phen)(py)\ Cl\ dppz]^{+}$ and $[Ru(phen)(py)_2dppz]^{2+}$ complexes were present in the minor groove. However, the elongation of the DNA, the prevention of the ethidium intercalation, and the binding stoichiometry could not be described by minor groove binding. Therefore, classical intercalation of dppz, and classical minor groove binding are conceivably rejected, and a new binding mode for $Ru(phen)(py)\ Cl\ dppz]^{+}$ and $[Ru(phen)(py)_2dppz]^{2+}$ may be proposed, where the dppz ligands were located inside the DNA, preventing the intercalation of ethidium while being protected from outside water molecules. However, the dppz ligands were strongly tilted, while the contour length of the DNA increased and the strength of the interactions with DNA bases remained. The structure of the DNA bases must have been strongly distorted for the large tilt of the dppz ligand to be possible within the DNA.

5. Conclusion

Replacing one of the two phenanthroline ligands of $[Ru(phen)_2dppz]^{2+}$ with two pyridine molecules or one pyridine molecule and a chloride ion resulted in strong deviation from the binding mode of $[Ru(phen)_2dppz]^{2+}$ to DNA. Therefore, both its phenanthroline ligands must be anchored to allow the classical intercalation of its dppz ligand.

Acknowledgement

The authors acknowledge the support from the National Research Foundation of Korea (2009-0083855).

References

[1] B. Nordén, P. Lincoln, B. Åkerman, E. Tuite, in: A. Sigel, B. Sigel (Eds.), Metal Ions in Biological System, Marcel Dekker, New York, 1996.
[2] J.K. Barton, Metals and DNA: molecular left-handed complements, Science 233 (1986) 727–734.
[3] J.K. Barton, C.V. Kumar, N.J. Turro, DNA-mediated photoelectron transfer reactions, J. Am. Chem. Soc. 108 (1986) 6391–6393.
[4] S. Delaney, J. Yoo, E.D.A. Stemp, J.K. Barton, Charge equilibration between two distinct sites in double helical DNA, Proc. Natl. Acad. Sci. U. S. A. 101 (2004) 10511–10516.
[5] C.J. Murphy, M.R. Arkin, Y. Jenkins, N.D. Ghatlia, S.H. Bossmann, N.J. Turro, J.K. Barton, Long-range photoinduced electron transfer through a DNA helix, Science 262 (1993) 1025–1029.
[6] C.J. Murphy, M.R. Arkin, N.D. Ghatlia, S. Bossmann, N.J. Turro, J.K. Barton, Fast photoinduced electron transfer through DNA intercalation, Proc. Natl. Acad. Sci. U. S. A. 91 (1994) 5315–5319.
[7] M.E. Núñez, J.K. Barton, Probing DNA charge transport with metallointercalators, Curr. Opin. Chem. Biol. 4 (2000) 199–206.
[8] C.R. Rreadway, M.G. Hill, J.K. Barton, Charge transport through a molecular p-stack: double helical DNA, Chem. Phys. 281 (2002) 409–428.
[9] B.W. Lee, S.J. Moon, M.R. Youn, J.H. Kim, H.G. Jang, S.K. Kim, DNA mediated resonance energy transfer from 4′,6-diamidino-2-phenylindole to [Ru(1,10-phenanthroline)$_2$L]$^{2+}$, Biophys. J. 85 (2003) 3865–3871.
[10] B.H. Yun, J.-O. Kim, B.W. Lee, P. Lincoln, B. Nordén, J.-M. Kim, S.K. Kim, Simultaneous binding of ruthenium(II) [(1,10-phenanthroline)$_2$dipyridophenazine]$^{2+}$ and minor groove binder 4′,6-diamidino-2-phenylindole to poly[d(A−T)$_2$] at high binding densities: observation of fluorescence resonance energy transfer across the DNA stem, J. Phys. Chem. B 107 (2003) 9858–9864.
[11] J.Y. Choi, J.-M. Lee, H.S. Lee, M.J. Jung, S.K. Kim, J.M. Kim, Mixing ratio-dependent energy transfer from DNA-bound 4′,6-diamidino-2-phenylindole to [Ru(1,10-phenanthroline)$_2$dipyrido[3,2-*a*:2′,3′-*c*]phenazine]$^{2+}$, Biophys. Chem. 134 (2008) 56–63.
[12] Y. Jenkins, A.E. Freidman, N.J. Turro, J.K. Barton, Characterization of dipyridophenazine complexes of ruthenium(II): the light switch effect as a function of nucleic acid sequence and conformation, Biochemistry 31 (1992) 10809–10816.
[13] C. Hirot, P. Lincoln, B. Nordén, DNA binding of DELTA- and LAMBDA-[Ru(phen) 2DPPZ]$^{2+}$, J. Am. Chem. Soc. 115 (1993) 3448–3454.
[14] I. Haq, P. Lincoln, D. Suh, B. Nordén, B.Z. Chowdhry, J.B. Chaires, Interaction of delta- and lambda- [Ru(phen)2 DPPZ] with DNA – a calorimetric and equilibrium binding study, J. Am. Chem. Soc. 117 (1995) 4788–4796.
[15] A. Greguric, I.D. Greguric, T.W. Hambley, J.R. Aldrich-Wright, J.G. Collins, Minor groove intercalation of Δ- [Ru(Me$_2$phen)dppz]$^{2+}$ to the hexanucleotide d(GTCGAC)$_2$, J. Chem. Dalton Trans. (2002) 849–855.
[16] E. Amouyal, A. Homsi, J.C. Chambron, J.P. Sauvage, Synthesis and study of a mixed-ligand ruthenium(II) complex in its ground and excited states: bis(2,2′-bipyridine) (dipyrido[3,2-*a* : 2′,3′-*c*]phenazine-N^4N^5)ruthenium(II), J. Chem. Soc. Dalton Trans. (1990) 1841–1845.
[17] Y.J. Jang, B.-H. Kwon, B.-H. Choi, C.H. Bae, M.S. Seo, W.W. Nam, S.K. Kim, Intercalation of bulky D, D- and K, K-bis-Ru(II) complex between DNA base pairs, J. Inorg. Biochem. 102 (2008) 1885–1891.
[18] A. Wada, S. Kozawa, Instrument for the studies of differential flow dichroism of polymer solutions, J. Polym. Sci. 2 (1964) 853–864.
[19] B. Nordén, M. Kubista, T. Kurucsev, Linear dichroism spectroscopy of nucleic acids, Q. Rev. Biophys. Chem. 25 (1992) 51–170.
[20] A. Rodger, B. Nordén, Circular Dichroism & Linear Dichroism, Oxford University Press, New York, 1997.
[21] M. Eriksson, B. Nordén, Linear and circular dichroism of drug-nucleic acid complexes, Method Enzymol. 340 (2001) 68–98.
[22] C. Hiort, B. Nordén, A. Rodger, Enantiopreferential DNA binding of [ruthenium(II) (1,10-phenanthroline)$_3$]$^{2+}$ studied with linear and circular dichroism, J. Am. Chem. Soc. 112 (1990) 1971–1982.
[23] P. Lincoln, A. Broo, B. Nordén, Diastereomeric DNA-binding geometries of intercalated ruthenium(II) trischelates probed by linear dichroism:[Ru (phen)$_2$DPPZ]$^{2+}$ and [Ru(phen)$_2$BDPPZ]$^{2+}$, J. Am. Chem. Soc. 118 (1996) 2644–2653.
[24] M. Ardhammar, P. Lincoln, A. Rodger, B. Nordén, Absolute configuration and electronic state properties of light-switch complex [Ru(phen)2d ppz]2+ deduced from oriented circular dichroism in a lamellar liquid crystal host, Chem. Phys. Lett. 354 (2002) 44–50.
[25] G. Cohen, H. Eisenberg, Viscosity and sedimentation study of sonicated. DNA-proflavin complexes, Biopolymers 8 (1969) 45–55.
[26] M. Chien, A.P. Grollman, S.B. Horwitz, Bleomycin–DNA interaction: fluorescence and proton resonance studies, Biochemistry 16 (1977) 3641–3647.
[27] J.-H. Moon, S.K. Kim, U. Sehlstedt, A. Rodger, B. Nordén, DNA structural features responsible for sequence-dependent binding geometries of Hoechst 33258, Biopolymers 38 (1996) 593–606.
[28] H.-K. Kim, J.-M. Kim, S.K. Kim, A. Rodger, B. Nordén, Interactions of intercalative and minor groove binding ligands with triplex poly(dA).[poly(dT)]2 and with duplex poly(dA).poly(dT) and poly[d(A-T)]2 studied by CD, LD and normal absorption, Biochemistry 35 (1996) 1187–1194.
[29] S. Eriksson, S.K. Kim, M. Kubista, B. Nordén, Binding of 4′,6-diamidino-2-phenylindole (DAPI) to AT regions of DNA: evidence for an allosteric conformational change, Biochemistry 32 (1993) 2987–2998.
[30] E. Tuite, B. Nordén, Intercalative interactions of ethidium dyes with triplex structures, Bioorg. Med. Chem. 3 (1995) 701–711.
[31] G.F. Loontiens, L.W. McLaughlin, S. Diekmann, R.M. Clegg, Binding of Hoechst 33258 and 4′,6-diamidino-2-phenylindole to self-complementary decadeoxynucleotides with modified exocyclic base substituents, Biochemistry 30 (1991) 182–189.